PHYSICAL REVIEW A VOLUME 48, NUMBER 5 NOVEMBER 1993

High-order harmonic-generation cutoff

Anne L'Huillier, M. Lewenstein,* P. Salières, and Ph. Balcou
Service des Photons, Atomes et Molécules, Centre d'Etudes de Saclay, 91191 Gif-sur-Yvette, France

M. Yu. Ivanov†
National Research Council of Canada, M-23A, Ottawa, Ontario, Canada K1A OR6

J. Larsson and C. G. Wahlström
Department of Physics, Lund Institute of Technology, S-22 100 Lund, Sweden
(Received 19 February 1993)

We have experimentally determined the harmonic-generation cutoff as a function of the laser intensity in neon using an intense, short-pulse Ti:sapphire laser. The experimental cutoff is lower than that obtained in single-atom calculations. Using a simple quantum-mechanical approach to harmonic generation valid at high intensity, we show that the difference is due to the effect of propagation.

PACS number(s): 42.65.Ky, 32.80.Rm

High-order harmonic generation has recently become one of the major topics of multiphoton physics. The spectrum of such radiation falls off for the first few harmonics, then exhibits a *plateau* extending sometimes to more than 150 eV [1,2]. The plateau ends up by a rather sharp *cutoff*. One of the most intriguing questions concerns the nature and location of this cutoff. Numerical calculations of Krause, Schafer, and Kulander, [3] have shown that the maximum energy at the end of the plateau, which we call the *cutoff energy*, is well approximated by the simple formula $I_p + 3U_p$, where I_p is the atomic ionization potential, while $U_p = \mathcal{E}^2/4\omega^2$ is the ponderomotive energy in the laser field of strength $\mathcal{E}$ and frequency ω. Some insight into the physical meaning of this formula has recently been given by Schafer, Kulander, and Krause [4] and by Corkum [5], using a two-step quasiclassical approach. In this model, electrons first tunnel through the barrier formed by the atomic potential and the laser field [6,7]. Their subsequent motion in the field is treated classically. Only those electrons that return to the nucleus can emit harmonics by recombining to the ground state. The maximum kinetic energy acquired by the electrons from the field at the time they return to the nucleus is $3.2U_p$, so that the maximum emitted energy is $I_p + 3.2U_p$, in accord with the prediction of [3].

The aim of this Rapid Communication is to discuss the harmonic-generation cutoff from experimental data to calculations involving the response of a single atom and of the macroscopic medium. We have performed systematic measurements of the harmonic-generation yields in neon using a short-pulse low-frequency laser. The experimental cutoff energy is found to be approximately $I_p + 2U_p$ and is therefore lower than that predicted in single-atom theories [3,8]. To understand the difference, we have investigated the influence of propagation [9] and in particular of focusing on the location of the cutoff. We use single-atom dipole moments obtained from a simple (and new) quantum-mechanical theory of harmonic generation valid in the tunneling limit. The results obtained for the response of the macroscopic medium agree well with the experimental data.

The experiments have been carried out with a 100-mJ Ti:sapphire laser operating at a wavelength of 794 nm and a pulse width of 250 fs. The laser is loosely focused by a $f = 2$ m lens into a 1-mm 20-Torr atomic beam provided by a pulsed gas jet. The confocal parameter (b) is measured to be 1.3 cm. The 10-Hz repetition rate allows us to perform systematic measurements of the harmonic-generation yields as a function of the laser intensity from 20 eV (the 13th harmonic) to about 130 eV (the 83rd harmonic, the highest observed with significant dynamical range). In Fig. 1, we present the results for seven of these harmonics. The harmonics appear successively as the intensity increases. They vary first rather rapidly with the laser intensity, in the cutoff region. Then, they reach the plateau, where all of the harmonics have approximately the same strength, exhibiting a slow dependence with the laser intensity. As the harmonic order increases, the variation in the cutoff region becomes more rapid and the variation in the plateau slower. The loca-

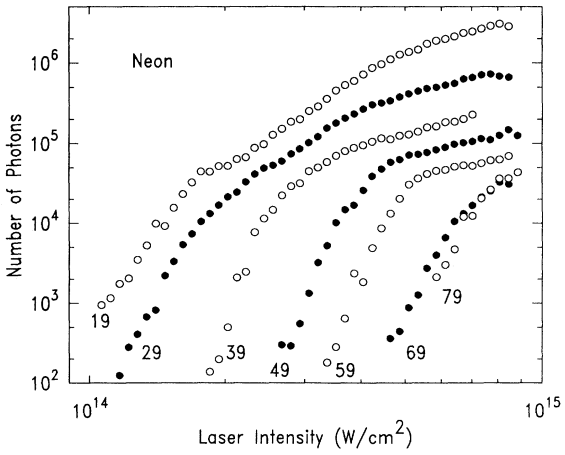

FIG. 1. 19th, 29th, 39th, 49th, 59th, 69th, and 79th harmonics in neon as a function of the laser intensity

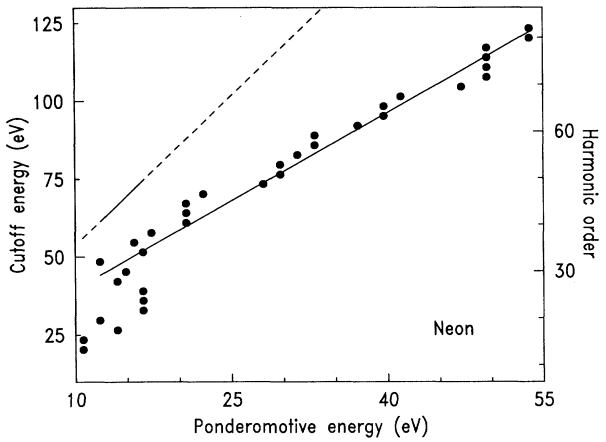

FIG. 2. Cutoff energy as a function of the ponderomotive energy. The solid line is a linear best fit, $21 + 2U_p$; the dashed line is the prediction of the single-atom response, $21.6 + 3.2U_p$.

tion of the change of slope indicates at which intensity a given harmonic reaches the plateau. The saturation intensity due to ionization is measured to be about 6×10^{14} W/cm^2. Our measurement of the laser intensity at best focus is accurate to within $\pm 50\%$. In order to get a more precise determination, we have performed ion measurements in the same chamber using a time-of-flight spectrometer. The measured intensity is only 25% smaller than that predicted by tunnel ionization [7]. We shall, however, correct our intensity by this factor in the following. Similar results have been obtained previously by Macklin, Kmetec, and Gordon [2].

In Fig. 2, we plot the harmonic order at which the cutoff occurs as a function of the laser intensity expressed in units of ponderomotive energy. This is done by locating the position of the change of slope in the intensity dependences for all of the harmonics, from the 13th to the 83rd. We also indicate on the left vertical scale, the harmonic photon energy, i.e., the cutoff energy. A linear regression performed on the harmonics higher than the 27th gives a cutoff law equal to approximately $21 + 2U_p$. For comparison, we show the single-atom prediction $21.6 + 3.2U_p$ by the dashed line. The cutoff law determined experimentally is significantly lower than that predicted by the single-atom results.

A theoretical description of harmonic-generation processes involves two steps: (i) the calculation of the harmonic emission by a single atom at the different intensities present in the nonlinear medium; (ii) the integration of the propagation equations for the harmonic fields created in the medium, using as a source the single-atom dipole moments calculated in the first step. Propagation effects have been previously shown not to affect much the single-atom spectra, but these calculations [9] had been performed in a completely different regime, i.e., for much lower intensities, of the order of 10^{13} W/cm^2 and for much lower orders (3 to 21).

To deal with the first step, i.e., to calculate in a simple way the single-atom dipole moments in this low-frequency high-intensity regime, we have developed a new quantum-mechanical theory of harmonic generation, valid in the tunnel ionization limit (when $U_p > I_p \gg \omega$, ω being the laser frequency) [7,6,10]. In this approach, we neglect the contribution of all excited bound states, the depletion of the ground state ($|0\rangle$), and the nonsingular off-diagonal part of the continuum-continuum dipole matrix elements [11] (which amounts to neglecting the influence of the ionic potential). The singular part of the continuum-continuum dipole matrix elements, $\langle \mathbf{v}|x|\mathbf{v}'\rangle = i\partial\delta(\mathbf{v}-\mathbf{v}')/\partial v_x$, treated exactly, describes the free-electron motion in the laser field (assumed to be linearly polarized in the x direction) [10]. The time-dependent wave function $|\Psi(t)\rangle$ takes the form $e^{iI_p t}[a(t)|0\rangle + \int d^3\mathbf{v}\, b(\mathbf{v},t)|\mathbf{v}\rangle]$, where $a(t) \simeq 1$ is the ground-state amplitude, and $b(\mathbf{v},t)$ are the amplitudes of the continuum states. The Schrödinger equation for $b(\mathbf{v},t)$ in the length gauge reads

$$\dot{b}(\mathbf{v},t) = -i\left(\frac{\mathbf{v}^2}{2} + I_p\right) b(\mathbf{v},t) - \mathcal{E}\cos(t)\,\frac{\partial b(\mathbf{v},t)}{\partial v_x} + i\mathcal{E}\cos(t)\, d_x(\mathbf{v}), \tag{1}$$

where $\mathcal{E}\cos(t)$ denotes the laser field (we use atomic units and set the photon energy ω to 1) and $d_x(\mathbf{v}) = \langle \mathbf{v}|x|0\rangle$ is the coupling to the continuum. The information about the atom is reduced to the form of $d_x(\mathbf{v})$ (assumed to have a Gaussian dependence in the calculations) and to the value of the ionization energy I_p. The x component of the time-dependent dipole moment is given by $x(t) = \int d^3\mathbf{v}\, d_x^*(\mathbf{v}) b(\mathbf{v},t)$, if we consider only the transitions back to the ground state [12]. We solve Eq. (1) exactly and insert the solution into the expression for $x(t)$. Introducing the canonical momentum $\mathbf{p} = \mathbf{v} + \mathbf{A}(t)$, where $\mathbf{A}(t)$ is the vector potential of the laser field, the dipole moment reads

$$x(t) = i\int_0^t dt' \int d^3\mathbf{p}\,\mathcal{E}\cos(t') d_x(\mathbf{p} - \mathbf{A}(t')) \times \exp\left[-i\int_{t'}^t dt''\{[\mathbf{p} - \mathbf{A}(t'')]^2/2 + I_p\}\right] \times d_x^*(\mathbf{p} - \mathbf{A}(t)) + \text{c.c.} \tag{2}$$

This equation can be interpreted semiclassically [13]. The first term in the integral $\mathcal{E}\cos(t')d_x(\mathbf{p} - \mathbf{A}(t'))$ is the probability amplitude for an electron to make a transition to the continuum at time t' with the canonical momentum $\mathbf{p}$. The electronic wave function is then propagated till the time t and acquires a phase factor equal to $\exp[-iS(\mathbf{p},t,t')]$, where $S(\mathbf{p},t,t')$ is the classical action. The effects of the atomic potential are assumed to be small between t' and t, so that $S(\mathbf{p},t,t')$ actually describes the motion of an electron freely moving in the laser field with a constant momentum $\mathbf{p}$. The electron recombines at time t with an amplitude equal to $d_x^*(\mathbf{p} - \mathbf{A}(t))$, which gives the last factor entering Eq. (2).

The major contribution to the integral in Eq.(2) comes from the stationary points of the classical action, which correspond to those momenta $\mathbf{p}$ for which the electron

born close to the origin at t' returns to the origin at t. The general form for the dipole moment $x(t)$ is $\int_0^\infty f(t,\tau)\exp[-iS(t,\tau)]\,d\tau$, where we have introduced the return time $\tau = t - t'$. $f(t,\tau)$ is a slowly varying function of t and τ, whereas

$$S(t,\tau) = (I_p + U_p)\tau - 2U_p(1-\cos(\tau))/\tau - U_p C(\tau)\cos(2t-\tau), \quad (3)$$

with $C(\tau) = \sin(\tau) - 2[1-\cos(\tau)]/\tau$, is the action corresponding to a return of the electron to the origin at time t after the interval τ. $S(t,\tau)$ is a linear function of $\sin(2t)$ and $\cos(2t)$, so that the Fourier components x_q of $x(t)$ can be simply expressed in terms of Bessel functions $J_K(U_pC(\tau))$, with $2K = q \pm 1, 3$. A lot of insight can be drawn from the analysis of the function $C(\tau)$, which determines the variation of $S(t,\tau)$ as a function of t. Maxima of $2U_p|C(\tau)|$ are equal to the maxima of the kinetic energy that the electron has gained from the field when it returns to the nucleus. The first maximum of $2|C(\tau)|$ is 3.17. The following ones are of the order of 2–2.4. Since the Bessel functions $J_K(x)$ become exponentially small when $x < K$, we conclude that the harmonic-generation cutoff for $U_p \gg I_p$ is at $3.17U_p$. In the range of $2U_p \leq 2K \leq 3.17U_p$ only the contributions from the first maximum are important. When $2K$ becomes smaller than $\sim 2U_p$, more and more maxima contribute, giving rise to interference effects.

This model, which can be generalized to more complex problems (e.g., the inclusion of the Coulomb potential or the treatment of arbitrary laser fields), has two advantages: it gives a lot of physical insight into these high-order harmonic-generation processes, recovering in particular the single-atom cutoff law [3,8] and the semiclassical interpretation of Refs. [4,5] in a quantum-mechanical formulation; moreover, the harmonic components of the single-atom dipole moment are simply calculated as single integrals over τ of expressions involving Bessel functions (as in [8]). Therefore, they are easy to handle in propagation calculations requiring the knowledge of the single-atom response over a fine intensity grid (sampling the nonlinear medium).

The propagation equations have been solved within the slowly varying envelope approximation and the paraxial approximation, following the method described in Ref. [9]. The macroscopic parameters characterizing the laser and the interaction have been chosen to mimic the experimental conditions. In Fig. 3, we plot the 35th harmonic intensity (in arbitrary units) as a function of $U_p = 5.9 \times 10^{-14} I$, where I, the laser intensity, is expressed in W/cm^2. The dashed line shows the single-atom response. In the cutoff region, i.e., at low intensity, the harmonic strength grows rather steeply. At the intensity such that $35\omega \simeq I_p + 3.2U_p$ (denoted $\alpha = 3.2$ in the figure), the harmonic enters the plateau region and becomes progressively dominated by interference effects. The solid line shows the result of the complete calculation. The effect of propagation is to shift the change of slope, indicating the position of the cutoff to a higher intensity, such that $35\omega \simeq I_p + 2U_p$ ($\alpha = 2$ in the figure), and to average out the interferences observed in the single-atom response. Finally, the full circles show the experimental results. We obtain a good agreement between the theoretical calculations including propagation and the experimental results.

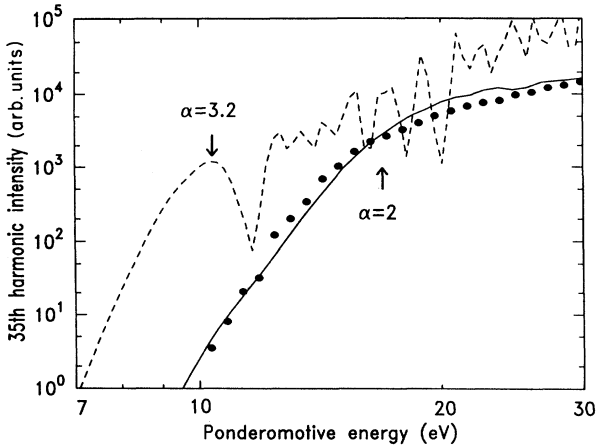

FIG. 3. 35th harmonic as a function of intensity, expressed in terms of the ponderomotive energy U_p. The single-atom and many-atom responses are indicated, respectively, by dashed and solid lines. The experimental data are shown by the full circles.

In these high-order harmonic-generation processes performed in neon at a relatively low pressure and at an intensity smaller than that needed to significantly ionize the medium, the main limitation to phase matching is due to focusing, i.e., to the phase mismatch introduced by the geometrical phase slip across the focus. The coherence length induced by focusing takes a simple form, $L_{\rm coh} = \pi b/2(q-1)$, where b is the laser confocal parameter and q the harmonic order. Focusing becomes a limitation to harmonic generation when $L_{\rm coh}$ is comparable to or smaller than the length of the medium L. Note the order dependence of $L_{\rm coh}$. Even for a very loosely focused laser beam, the geometry is of a tight-focused type for harmonics of order $q > \pi b/2L$. In our experiment, $b \approx 1.3$ cm, $L = 1$ mm, so that tight focusing begins approximately at the 21st harmonic. In order to understand better the effect of propagation on the harmonic-generation cutoff, we have performed a series of calculations in which we have varied the laser confocal parameter, from a loose to a tight-focusing geometry for two harmonics, the 35th and the 71st. The results are presented in Fig. 4. The dashed lines are the single-atom results. The solid lines have been obtained, from the top to the bottom, for $b = 3,1.5,1,0.5$ cm in Fig. 4 (35th harmonic) and $b = 5,3,2,1$ cm in Fig. 4 (71st harmonic). In both cases, as one goes from a loose to a tight-focusing geometry, the location of the change of slope indicating the position of the cutoff switches rather abruptly from $\alpha = 3.2$ to $\alpha \approx 2$ (with a slightly higher value for the 71st harmonic). This occurs at approximately $b = 1.5$ cm for the 35th harmonic and $b = 3$ cm for the 71st harmonic, which corresponds to $L_{\rm coh} = 0.7L$.

In a tight-focusing geometry, phase matching depends

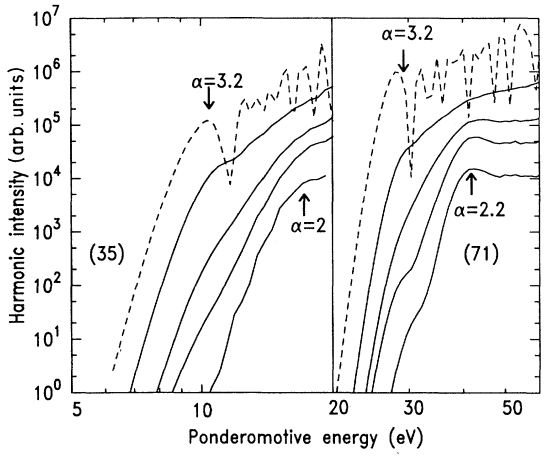

FIG. 4. 35th and 71st harmonics as a function of the laser intensity. The dashed lines indicate the single-atom response; the solid lines are results obtained by including the effect of propagation in different geometries. From the top to the bottom, b = 3,1.5,1,0.5 cm (35th harmonic); b = 5,3,2,1 cm (71st harmonic).

strongly on the variation of the polarization with intensity [9]. When this variation is rapid, as is the case in the cutoff region, the polarization is mostly concentrated close to the focus, with maximum cancellation effects between the field created before and after the focus and poor phase matching. When the harmonic reaches the plateau, the single-atom emission rate saturates, decreases, and exhibits oscillations. Consequently, the volume of emitting dipoles increases considerably, leading to reduced cancellation effects and much more efficient phase matching. Simultaneously the spatial profile becomes strongly distorted, as recently reported by Tisch *et al.* [14]. The curves corresponding to the smallest confocal parameters show three regions. At low intensity, there is a rapid increase due to the rapid increase in the single-atom response. At intermediate intensities (between $\alpha = 3.2$ and $\alpha = 2$), there is a second increase due to the rapid increase in the phase matching (whereas the single-atom response saturates). Finally the curve saturates at α=2, when both the phase matching and the single-atom response saturates. The experimental results will show only the most pronounced change of slope, i.e., the one at $\alpha = 2$. In conclusion, we have shown that the apparent discrepancy between single-atom theoretical predictions and experimental results can be explained by the effect of phase matching in a tight-focusing geometry.

We are grateful to K. C. Kulander, K. J. Schafer, and P. B. Corkum for helpful discussions. One of us (M.L.) thanks the SPAM in Saclay for hospitality and for financial support. Financial support from the Swedish National Science Research Council is acknowledged.

* Permanent address: Centrum Fizyki Teoretycznej PAN, Al. Lotników 32/46, 02-668 Warsaw, Poland.

† Permanent address: General Physics Institute, Vavilov Str. 38, Moscow 117942, Russia.

[1] A. L'Huillier and Ph. Balcou, Phys. Rev. Lett. **70**, 774 (1993).

[2] J. J. Macklin, J. D. Kmetec, and C. L. Gordon III, Phys. Rev. Lett. **70**, 766 (1993).

[3] J. L. Krause, K. J. Schafer, and K. C. Kulander, Phys. Rev. Lett. **68**, 3535 (1992).

[4] K. J. Schafer, K. C. Kulander, and J. L. Krause (unpublished).

[5] P. B. Corkum (unpublished).

[6] L. V. Keldysh, Zh. Eksp. Teor. Fiz. **47**, 1945 (1964) [Sov. Phys. JETP **20**, 1307 (1965)]; F. Faisal, J. Phys. B **6**, L312 (1973); H. R. Reiss, Phys. Rev. A **22**, 1786 (1980).

[7] M. V. Ammosov, N. B. Delone, and V. P. Kraïnov, Zh. Eksp. Teor. Fiz. **91**, 2008 (1986) [Sov. Phys. JETP **64**, 1191 (1986)].

[8] W. Becker, S. Long, and J. K. McIver, Phys. Rev. A **41**, 4112 (1990).

[9] A. L'Huillier, Ph. Balcou, S. Candel, K. J. Schafer, and K. C. Kulander, Phys. Rev. A **46**, 2778 (1992).

[10] J. Grochmalicki, J. R. Kukliński, and M. Lewenstein, J. Phys. B **19**, 3649 (1986).

[11] M. Y. Ivanov and K. Rzążewski, J. Mod. Opt. **39**, 2377 (1992).

[12] J. L. Krause, K. J. Schafer, and K. C. Kulander, Phys. Rev. A **45** 4998 (1992).

[13] N. B. Delone and V. P. Kraïnov, *Atoms in Strong Fields* (Springer-Verlag, Heidelberg, 1985).

[14] J. W. G. Tisch, R. A. Smith, M. Ciarrocca, J. P. Marangos, and M. H. R. Hutchinson (unpublished).